Published in final edited form as:
Stem Cells. 2011 July ; 29(7): 1052–1063. doi:10.1002/stem.662.

Development of histocompatible primate induced pluripotent stem cells for neural transplantation

Michela Deleidi, **Gunnar Hargus**, **Penelope Hallett**, **Teresia Osborn**, and **Ole Isacson***
Center for Neuroregeneration Research, Harvard Medical School/McLean Hospital, Belmont, MA, 02478; Udall Parkinson's Disease Research Center of Excellence; Harvard Neurodiscovery Center, Boston, Massachusetts 02114, USA.

Abstract

Immune rejection and risk of tumor formation are perhaps the greatest hurdles in the field of stem cell transplantation. Here, we report the generation of several lines of induced pluripotent stem cells (iPSCs) from Cynomolgus macaque (CM) skin fibroblasts carrying specific major histocompatibility complex (MHC) haplotypes. In order to develop a collection of MHC-matched iPSCs, we genotyped the MHC locus of 25 CM by microsatellite PCR analysis. Using retroviral infection of dermal skin fibroblasts, we generated several CM-iPSC lines carrying different haplotypes. We characterized the immunological properties of CM-iPSCs and demonstrated that CM-iPSCs can be induced to differentiate in vitro along specific neuronal populations, such as midbrain dopaminergic (DA) neurons. Midbrain-like DA neurons generated from CM-iPSCs integrated into the striatum of a rodent model of Parkinson's disease (PD) and promoted behavioral recovery. Importantly, neither tumor formation nor inflammatory reactions were observed in the transplanted animals up to six months after transplantation. We believe that the generation and characterization of such histocompatible iPSCs will allow the pre-clinical validation of safety and efficacy of iPSCs for neurodegenerative diseases and several other human conditions in the field of regenerative medicine.

Keywords

Parkinson's disease; stem cells; transplantation; non-human primates

Introduction

One of the major obstacles in the field of regenerative medicine is the need for immunosuppressive treatments in order to prevent graft rejection and graft versus host disease (GVHD). The recent advances in the field of cell reprogramming and the generation of patient-specific induced pluripotent stem cells (iPSCs) can theoretically overcome such limitations by allowing autologous transplants[1–3]. Dermal fibroblasts are currently the most common tissue source for the generation of iPSCs. Such somatic cells are easily obtained by non-invasive skin biopsies and iPSCs can be derived and differentiated into several lineages without the ethical concerns of embryonic stem cells (ESCs). With respect to cell therapy,

*Manuscript correspondence: Prof. Ole Isacson, Harvard Medical School/McLean Hospital, MRC 1, Belmont, MA 02478, Tel. 1-617-855-3283, Fax. 1-617-855-2522, ole_isacson@hms.harvard.edu.

Contributions

M.D.: Conception and design, collection and/or assembly of data, data analysis and interpretation, manuscript writing, final approval of manuscript; G.H., P.H., T.O.: collection and/or assembly of data, final approval of manuscript; O.I.: Conception and design, grant support, data analysis and interpretation, manuscript writing, final approval of manuscript.

Disclosure of Potential Conflicts of Interest: the authors indicate no potential conflicts of interest.

iPSC technology could also provide an alternative to ESCs for the generation of a human leucocyte antigen (HLA)-haplotyped bank of pluripotent stem cell lines for clinical applications[4]. Nonhuman primates (NHP) are important models for major human diseases, including neurodegenerative diseases, and transplantation research[5, 6]. Mauritian Cynomolgus macaques (CM) (*Macaca fascicularis*) exhibit limited MHC diversity, and almost all of the MHC genetic diversity in this population is distributed among seven haplotypes (H1–H7)[7]. Specific CM MHC haplotypes can be identified by genetic screening using a panel of microsatellite markers[8]. The generation of MHC-matched iPSCs from NHP would therefore be of great value for immunological research and pre-clinical validation of histocompatible iPSCs in regenerative medicine.

Immunological reactions also occur in "immune-privileged" organs such as the central nervous system. The activation of the innate and adaptive immune system in the brain can interfere with the functional engraftment of the transplanted neurons. The generation of patient-specific iPSCs can overcome such limitations by allowing autologous transplants and the establishment of histocompatible stem cell banks. The first necessary step toward the clinical use of such iPSCs is the generation of NHP iPSCs and the characterization of the immunogenicity, tumorigenicity, and functional relevance of their neuronal derivatives in experimental models of neurodegenerative diseases. Here we describe the generation of a collection of histocompatible NHP iPSCs, and their functional validation in rodent models of Parkinson's disease (PD).

Material and Methods

Animals

Adult female Sprague-Dawley rats (200–250 g) were purchased from Charles River (Wilmington, MA). Female Sprague-Dawley rats with a unilateral 6-hydroxydopamine (6-OHDA) lesion were obtained from Taconic (Taconic Farms Inc., Germantown, NY). Four adult male Mauritian CM were used to obtain skin biopsies[9, 10]. All animal procedures were performed in accordance with the guidelines of the National Institutes of Health and approved by the Institutional Animal Care and Use Committee (IACUC) at McLean Hospital and the New England Regional Primate Research Center, Harvard Medical School.

MHC cloning and sequencing

Prospective MHC typing was performed at Wisconsin National Primate Research Center, (University of Wisconsin, Madison), as described[8].

Fibroblast cell culture

Dermal fibroblasts from an Indonesian CM were purchased from Coriell Cell Repositories (Camden, NJ). Fibroblasts were generated from explants of 3 mm dermal biopsies obtained from Mauritian CM. Dermal pieces were incubated for 2 hrs with 1000 U/ml collagenase B (Roche, Indianapolis, IN) at 37°C. Cells were replated in growth medium [Dulbecco's modified eagle medium (DMEM, Thermo Scientific HyClone, Waltham, MA), 10% fetal bovine serum (FBS, Invitrogen, Carlsbad, CA)]. After 2 weeks, fibroblast outgrowths from the explants were passaged with 0.05% trypsin.

Peripheral blood mononuclear cell isolation

PBMCs were isolated by centrifugation over a 95% Ficoll-Paque™ PLUS (GE Healthcare Life Sciences, Piscataway, NJ) gradient and re-suspended in RPMI 1640 medium (GIBCO, Invitrogen) supplemented with 10% FBS.

Generation of cynomolgus macaque induced pluripotent stem cells

Human OCT4, SOX2 and KLF4, c-MYC retroviral vectors were obtained from Addgene (Cambridge, MA). To generate virus, 293T cells in 10-cm plates were transfected with 2.5 μg of retroviral vector, 0.25 μg of VSV-G vector and 2.25 μg of Gag-Pol vector. Two days after transfection, supernatants were filtered and centrifuged. To produce monkey iPSCs, 1×10^5 fibroblasts were plated in one well of a six-well plate and infected with retrovirus (MOI=10) with 8μg/mL polybrene (Sigma-Aldrich, St. Louis, MO). Three days after infection, cells were split into plates pre-seeded with mouse embryonic fibroblasts (MEF, GlobalStem, Rockville, MD). Medium was changed to hESC medium 5 days after infection. CM-iPSCs and human ESCs were grown according to standard protocols[11]. All experiments were approved by the Partners Embryonic Stem Cell Research Oversight (ESCRO) Committee under protocol number 2006-04-001A.

Alkaline phosphatase detection and immunocytochemistry

Alkaline phosphatase detection (AP) staining was performed using Alkaline Phosphatase Detection Kit (Chemicon, Temecula, CA), according to the manufacturer's instructions. For immunocytochemistry, cells were fixed in 4% paraformaldehyde for 10 minutes, rinsed with PBS, and blocked by 10% donkey serum in PBST (PBS+0.1% TritonX-100) for 60 minutes. Immunofluorescent staining was performed as previously described[12]. Primary antibodies included SSEA-4 (1:500, DSHB, Iowa City, IA), TRA-1–60 (1:50, Chemicon), TRA-1–81 (1:50, Chemicon), NANOG (1:100, R&D systems, Minneapolis, MN), Oct-4 (1:100, Santa-Cruz Biotechnology, Santa Cruz, CA), β-TubIII (1:1000, Chemicon), TH (1:1000, Pel-Freez Biologicals, Rogers, AR), FOXA2 (1:100, Santa-Cruz Biotechnology).

Karyotyping

G-banding chromosomal analysis was performed by Cell Line Genetics (Madison,WI).

Teratoma formation and analysis

Teratoma assay was performed by Applied Stem Cell (Menlo Park, CA). iPSCs were harvested by 1mg/ml dispase. iPSCs were collected by centrifugation and resuspended in 50% Matrigel. 1×10^6 iPSCs were injected under the kidney capsule of NOD-SCID mice. Tumors developed within 4–8 weeks and teratomas were isolated after sacrificing the mice and fixed in formalin. After sectioning, teratomas were diagnosed based on hematoxylin and eosin staining.

In vitro differentiation

In vitro DA neuronal differentiation was performed as previously described[13]. Briefly, neural differentiation was induced by co-culture on a stromal feeder cell line (MS5) with the addition of 300ng/ml noggin for 21 days (R&D Systems, Inc., Minneapolis). Stem cells were cultured for 14 days in serum replacement medium [KnockOutTM DMEM supplemented with 15% KnockOutTM Serum Replacement, 1mM glutamine and 1% nonessential amino acids (all from Invitrogen, Carlsbad, CA)], followed by 7 days of culture in N2-medium consisting of DMEM/F12 (Invitrogen) supplemented with N2-A (Stem Cell Technologies; Vancouver, BC, Canada). At day 21, rosette structures were manually picked and plated on poly L-ornithine/laminin (Sigma-Aldrich) coated culture dishes. DA differentiation was induced by culturing cells for 16 days in N2-medium containing 200 ng/ml N-terminal fragment of Shh (R&D Systems), 100 ng/ml murine FGF8-b (R&D Systems), 20 ng/ml BDNF (PeproTech EC Ltd., London) and 200 μM ascorbic acid (Sigma-Aldrich). Cells were terminally differentiated in N2 medium containing dibutyryl cAMP (1 mM, Sigma–Aldrich), 200 μM ascorbic acid, 1ng/mL TGFβ3 (Calbiochem, San Diego), 20 ng/

mL GDNF (Sigma-Aldrich),100 ng/mL Wnt5a (R&D system), 20 ng/mL FGF2 (Invitrogen), 100 ng/mL FGF20 (Peprotech), 20 ng/ml BDNF (Peprotech) for 5 days.

Quantitative Real-Time PCR

Total RNA was extracted with an RNeasy kit (QIAGEN) as described[14]. The expression level of each gene was normalized to endogenous β-actin. Fold-change in gene expression was calculated using 2-ΔΔCT method[15]. All the results are from three technical replicates of three independent experiments. Primer sequences are available upon request.

Flow Cytometry Analysis

Flow cytometry was performed as previously described[16]. The following antibodies and their respective isotype controls were used: HLA-A, B, C; HLA-DP, DQ, DR and CD16 (BD-Pharmingen, San Diego, CA). Flow cytometric analysis was performed on a fluorescence-activated cell sorter FACSAria using FACSDiva software (BD Biosciences) and data were analyzed using FlowJo software (Tree Star, Ashland, OR). In some conditions, 25 ng/ml recombinant human IFN-γ (R&D systems) was added to the culture medium and cells analyzed after 2 days.

Transplantation into naïve rats and 6-Hydroxydopamine-lesioned rats

Five days after changing into the final differentiation media, cells were trypsinized and resuspended in HBSS containing 10 μg/ml GDNF at a density of 100,000 cells/μL. Unlesioned rats received 200,000 cells as 1 deposit at the following coordinates from bregma: AP +0.4; ML −3; DV −5.0. 6-OHDA lesioned rats were grafted into the striatum with 4 μl of cell suspension as 2 deposits of 200,000 cells using the following coordinates from bregma: site 1: AP +0.4; ML −3; DV −5.0; site 2: AP −0.5; ML −3.6; DV −5.0. Cells were engrafted at a rate of 0.3 μl per minute. Rats were immunosuppressed with cyclosporin A (10 mg/kg/day, Sandimmune, Sandoz, East Hannover, NJ). Rotational asymmetry of 6-OHDA-lesioned rats was analyzed after i.p. injection of amphetamine (4 mg/kg; 90 min) or s.c. injection of apomorphine (0.1 mg/kg; 40 min) two weeks before transplantation and at 4, 8, 12, 16 and 24 weeks after transplantation.

Histological and stereological procedures

Immunofluorescent staining was performed as previously described[13]. The following primary antibodies were used: sheep/rabbit anti-TH (1:1000, Pel-Freez Biologicals), rabbit anti-Pitx3 (1:250, Chemicon), goat/mouse anti-Foxa2 (1:100, Santa Cruz Biotechnology), rabbit/chicken anti-β−TubIII (1:1000, Tuj1, Covance, Princeton, New Jersey), rabbit anti-GFAP (1:1000, DAKO, Carpinteria, CA), mouse anti-SSEA-4 (1:500; DSHB), mouse anti-Oct4 (1:100, Santa Cruz Biotechnology), mouse anti-Calbindin (1:2000, Swant, Bellinzona, Switzerland), rabbit anti-Ki-67 (1:1000, Vector Laboratories, Burlingame, CA), rabbit anti-Iba1 (1:200, Wako, Osaka, Japan), rabbit anti-Girk2 (1:80, Alomone Labs Ltd, Jerusalem, Israel), mouse anti-hNCAM clone Eric1 (1:100, Santa Cruz Biotechnology), mouse anti-human-syntaxin (1:50, Chemicon). For light microscopy, biotinylated secondary antibodies (1:300, Vector Laboratories) were applied to detect anti-TH and anti-hNCAM antibody, followed by incubation in streptavidin-biotin complex (Vectastain ABC Kit Elite; Vector Laboratories) for 1h and visualized by incubation in 3,3´- diaminobenzidine (DAB; Vector Laboratories). Confocal analysis was performed using a Zeiss LSM510/Meta Station (Thornwood). Stereology was performed using Stereo Investigator image-capture equipment and software (MicroBright-Field,) and a Zeiss Axioplan I fluorescent microscope. Graft volumes were calculated using the Cavalieri estimator probe. The coefficient of error was used to assess probe accuracy and $P < 0.05$ was considered acceptable. Cell counts of TH^+ neurons were performed on every sixth (TH) section using an Axioplan microscope (Zeiss)

under a 20× lens. Counts from serial sections were corrected and extrapolated for whole graft volumes using the Abercrombie method[17]. Co-expression of Ki-67/hNCAM, FOXA2/TH and Pitx3/TH was assessed in random fields in all available sections containing the graft within one series.

Statistical analysis

Data are expressed as mean + SEM. Comparisons between the groups were performed using one-way Anova, and the effect of the graft on amphetamine rotation over time was evaluated using repeated-measures Anova. A simple regression analysis was performed to evaluate correlation between TH^+ neurons and behavioral recovery. Based on the results reported in our previous publications[13, 18, 19], only animals with grafts containing TH+ neurons (≥500) were included in the analysis. Significance was considered for $P<0.05$.The Statistical Package GraphPad Prism version 4.00 (GraphPad Software, San Diego California USA) was used to analyze the data.

Results

Microsatellite genotyping of Mauritian Cynomolgus macaques

In order to generate CM-iPSC lines fully or partially matched for MHC alleles, 25 Mauritian CM in our cohort were genotyped for the seven common MHC haplotypes (H1–H7) using microsatellite-based PCR[9,20, 21]. Such genetic analysis revealed that H1 and H3 were the most common haplotypes among this cohort of animals (32%), followed by H2 (28%) (Supplementary Fig. 1). Haplotype H7, a rare Mauritian haplotype (frequency <1%), was found in one animal in the current study. Thirty-six percent of the haplotypes were simple recombinants of two or three of the six major haplotypes (Supplementary Fig. 1).

Generation of isogenic Cynomolgus macaque induced pluripotent stem cells

Primary skin cells were isolated by biopsy from 4 CM (MF 27-04, MF 25-04, MF 95-06 and MF 66-02) (Supplementary Table 1). Dermal fibroblasts from an Indonesian CM (MF 01) were also used in this study. The class IA region of the H1, H2 and H3 haplotypes only differs by a single amino acid residue in the signal peptide that is cleaved from the mature class I protein[8]. These class I alleles are therefore considered functionally equivalent[8]. Based on the MHC haplotype frequency in our cohort, we predicted that generating iPSCs from MF 66-02 and MF 95-06 would provide a full match for 20% of recipients (MHC identical), a beneficial match for 60% of recipients (shared haplotype) and MHC-I match for 28% of recipients (MHC-I identical) (Supplementary Fig. 1). Transgenes encoding human KLF4, SOX2, OCT4, and c-MYC were introduced into fibroblasts by means of vesicular stomatitis virus glycoprotein (VSVg)–pseudotyped Moloney-based retroviruses. Three days after infection, the fibroblasts displayed morphological changes and were replated onto irradiated mouse embryonic fibroblast feeders (MEF). Six to eight weeks after infection, a small number of colonies with an ESC-like morphology with high nucleus-to-cytoplasm ratio and prominent nucleoli were identified and manually picked (Fig. 1A–C). From each well (1×10^5 cells), approximately 5 colonies were obtained (0.005% reprogramming efficiency). Colonies were manually picked every 7 days and displayed growth rates comparable to that of human ESCs and human iPSCs. Such colonies were propagated up to twenty passages. To demonstrate CM-iPSCs pluripotency in vitro, we stained colonies for pluripotency markers. All the clones stained positive for Nanog, Oct4, SSEA4, TRA-1–60 and TRA-1–81 (Fig. 1D). Colonies were also positive for Alkaline Phosphatase (AP) (Fig. 1E). CM-iPSCs lines maintained a normal karyotype over several passages (Fig. 1F). RT-PCR analyses performed using primers specific to the retroviral transcripts demonstrated complete silencing of viral transgenes, and reactivation of the endogenous loci (Fig. 1G).

Microsatellite analysis confirmed that CM-iPSCs maintained the HLA haplotype of the parental fibroblasts after viral-mediated reprogramming (Supplementary Fig. 2).

To demonstrate pluripotency in vivo, three CM-iPSC lines (MF 01, MF 27-04, MF 25-04; 1×10^6 cells) were injected under the kidney capsule of nonobese diabetes/severe-combined immunodeficient (NOD/SCID) mice (Supplementary Table 2). All iPSC lines formed teratomas within 4–8 weeks, which were comprised of tissues developing from all embryonic germ layers including glands and ducts (endoderm), adipose tissue, blood vessels, skeletal muscle and smooth muscle (mesoderm), neural rosettes and pigmented neural epithelium (ectoderm) (Supplementary Fig. 3).

Immunological characterization of Cynomolgus macaque induced pluripotent stem cells

We next characterized the expression of surface immunological markers on undifferentiated CM-iPSCs and their neural derivatives, including neural precursors (NP) and differentiated neurons. Expression of MHC-I and MHC-II proteins was analyzed by flow cytometry using antibodies directed against CM HLA-A/B/C and CM HLA-D/DQ/DR, respectively. Natural killer cells (NK) were analyzed by using an antibody against the NK-receptor CD16. The analysis of the immunophenotype of human ESCs (hESCs, H9) was also performed. Our analysis showed that undifferentiated CM-iPSCs and human ESCs express very low levels of MHC-I (Supplementary Fig. 4). MHC-II and CD16 were not detected on undifferentiated cells (Supplementary Fig. 4). We then examined the influence of interferon gamma (IFN-γ) treatment on the expression of such immune molecules. IFN-γ is a pro-inflammatory cytokine, member of type II class of interferons. It has several biological properties in the course of innate and adaptive immune responses, one of which is the increased expression of MHC-I and -II proteins. CM-iPSCs and hESCs were treated with 25 ng/mL IFN-γ. Expression of MHC-I, MHC-II and CD16 was analyzed after 48 hours by flow cytometry. Our analysis revealed that both CM-iPSCs and hESCs increased MHC-I expression upon IFN-γ treatment (Supplementary Fig. 4). However, differences were detected among different iPSC lines (Supplementary Fig. 4). Interestingly, the increase of MHC-I after IFN-γ was more evident in hESCs (Supplementary Fig. 4). IFN-γ induced a small increase of CD16 expression in hESCs but not in CM-iPSC lines. IFN-γ treatment did not affect MHC-II expression in any of the lines (Supplementary Fig. 4).

We next investigated whether neuronal differentiation influences the expression of MHC-I, MHC-II and CD16. CM-iPSCs were differentiated according to the stromal feeder cell-based differentiation protocol with some modifications[13, 22] (Fig. 2A). NP [stage 1, day in vitro (DIV) 27] and fully differentiated neurons (stage 2, DIV 42) were harvested for FACS analysis. NP and differentiated neurons expressed levels of MHC-I higher than undifferentiated cells (Supplementary Fig. 5). IFN-γ treatment increased MHC-I expression on NP and neurons (Supplementary Fig. 5). Differences in the response to IFN-γ were detected among different lines (Supplementary Fig. 5). MHC-II and CD16 were affected neither by neuronal differentiation nor IFN-γ treatment.

In vitro differentiation of CM-iPSCs into DA neurons

We next investigated the potential of 4 CM-iPSC lines (MF 01, MF 27-04, MF 25-04 and MF 95-06) to differentiate into DA neurons in vitro, using a protocol described in our published work showing the generation of midbrain-like DA neurons from parthenogenetic primate ESCs[13] (Fig. 2A). At the end of the differentiation protocol (DIV 42), cultures were stained for tyrosine hydroxylase (TH) and neuron-specific class III-β-tubulin (β-TubIII$^+$) to label DA neurons. CM-iPSCs generated neural rosettes at DIV 21(Fig. 2C) and DA neurons at DIV 42 (Fig. 2D–F). However we detected some differences in the number of total β-TubIII$^+$ neurons and TH$^+$ cells (MF 01, β-TubIII$^+$ 34±4.2%, TH$^+$ 2.8±1.3; MF 27-04, β-

TubIII$^+$ 35±3.5%, TH$^+$ 5.1±0.9%; MF 25-04, β-TubIII$^+$ 29±2.1%, TH$^+$ 2.5±1.2; MF 95-06, β-TubIII$^+$ 36±1.4%, TH$^+$ 4.9±2.4%) (Fig. 2B). Such variability is in line with the variability among different human iPSC lines[23]. Differentiated TH+ neurons expressed the midbrain marker FOXA2 (Fig. 2G). Quantitative RT-PCR further confirmed expression levels of midbrain DA markers in differentiated cultures such as FOXA2, vesicular monoamine transporter (VMAT), calbindin, aldehyde dehydrogenase 2 (ALDH), aromatic-L-amino acid decarboxylase (ADDC) and En1 (Fig. 2H).

Transplantation of iPSC-derived DA neurons into the striatum of naïve rats

We have recently shown that human iPSCs derived from healthy subjects and idiopathic PD patients survive upon transplantation in the striatum of naïve rats, and reveal a specific and reproducible pattern of neuronal outgrowth and targeting of long-distance brain areas 4 weeks after transplantation[23]. Such short-term in-vivo bioassay was therefore utilized to screen the capability of differentiated CM-iPSC neurons to survive and project after transplantation. CM-iPSCs were differentiated as described above, harvested at DIV 42, and 200,000 cells were transplanted into the right striatum of naïve rats under immunosuppression (n=7). Brains were analyzed 4 weeks after transplantation. Immunohistochemical analysis for the human specific neural adhesion molecules (hNCAM) revealed surviving grafts in all the transplanted animals (Fig. 3A–C). Interestingly, grafted neurons exhibited a pattern of outgrowth similar to the pattern we have recently described for human iPSC-derived neurons, showing projecting axons into the host striatum (Fig. 3D), along white matter tracts (e.g. corpus callosum) and into specific close and remote gray matter target areas (Fig. 3E–F)[23]. Immunostaining for the ionized calcium-binding adaptor molecule 1 (Iba1) revealed the absence of microglia reaction around the grafts (Fig. 3G). Iba1 is a Ca2+-binding peptide selectively expressed in microglia/macrophages, and participates in a variety of pathogenic processes in the mammalian brain and in chronic transplant rejection[24]. Immunostaining with antibodies to the lymphocyte marker CD3 revealed the absence of T-cell infiltration. Neither graft overgrowth nor tumors were observed 4 weeks after transplantation. To evaluate proliferation in the grafts we examined Ki-67 immunoreactivity in the brain of representative animals (Fig. 3H). Within the grafts, between 0.5–3% of the cells were Ki-67$^+$ indicating that the majority of transplanted cells were not proliferative in vivo by 4 weeks. All the grafts stained negative for Oct4 showing the absence of residual undifferentiated iPSCs (Fig. 3H).

Transplantation of CM-iPSC-derived DA neurons into the striatum of hemiparkinsonian rats

In order to validate the CM-iPSCs for future preclinical application into NHP, we next transplanted 400,000 differentiated CM-iPSCs (line MF 01) into the dorso-lateral striatum of 6-OHDA-lesioned rats, an animal model of PD (transplanted rats n=9, lesioned non-transplanted rats n=4). Amphetamine and apomorphine response were examined before and at 4, 8, 12 and 16 weeks post-transplantation (Fig. 4A). Animals showed a progressive decline in ipsilateral rotations starting at 12 weeks after transplantation ($p< 0.05$, compared to non-transplanted rats) (Fig. 4A). Grafts were analyzed histologically 16 weeks after transplantation. All animals had surviving grafts at post mortem analysis (Fig. 4B) as revealed by immunostaining for hNCAM. All the grafts had surviving TH+ neurons (1686.7±654.3) and showed partial reinnervation of the host striatum (Fig. 4B–G). All TH+ neurons were co-localized with the human/primate-specific marker NCAM clone eric1 (Fig. 5D,F). The degree of behavioral recovery significantly correlated with the number of surviving TH$^+$ neurons ($r=0.885$, $r^2=0.784$, $P=0.01$) (Fig. 5I). No graft overgrowth was observed in transplanted animals up to 4 months after transplantation. Immunostaining for the proliferation marker Ki-67 revealed the absence of proliferating cells within the grafts (Fig. 5C). We then analyzed whether the neuronal grafts induced astroglial or microglial

activation. Immunostaining for the microglial marker Iba1 and the astrocytic marker GFAP showed microglial cells with a resting phenotype and a few astrocytes around the grafts (Fig. 5A–B). Immunostaining with antibodies to the lymphocyte markers CD3, CD4 and CD8 revealed the absence of T-cell infiltration (data not shown).

We next analyzed the phenotype of the engrafted neurons. A subset of TH+ neurons co-expressed GIRK-2 and the transcription factors FOXA2 (30±4.6%) (Fig. 5E) and PITX3 (11±2.4%) (Fig. 5F), which are co-expressed with TH in midbrain DA neurons in the substantia nigra pars compacta (SNc)[25, 26]. We also found that a subset of TH^+ neurons coexpressed calbindin (Fig. 5G). Calbindin is expressed preferentially by the medial midbrain DA neuron subpopulations projecting to limbic territories, and not in the ventral mesencephalic subpopulation mostly affected in PD[25]. In order to verify the formation of mature synapses on grafted neurons we stained brains for human syntaxin. Immunostaining for TH and human syntaxin revealed a punctate synaptic expression pattern of syntaxin within the grafts and in the host striatum (Fig. 5H).

In order to confirm the long-term survival, safety and functional efficacy of CM-iPSCs, we then transplanted 6-OHDA lesioned rats with differentiated DA neurons generated from a different CM-iPSC line (line MF 27-04) (transplanted rats n=11, lesioned non-transplanted rats n=6). Amphetamine and apomorphine responses were examined before and at 4, 8, 12, 16 and 24 weeks post-transplantation (Fig. 6A–B). Analysis of amphetamine-induced behavior showed a significant reduction of clockwise rotations at 12 weeks after transplantation (Fig. 6A), indicating significant restoration of function caused by the 6-OHDA lesion ($p \leq 0.05$, $p \leq 0.01$, $p \leq 0.05$, compared to non-transplanted rats at 12, 16 and 24 weeks respectively). We found that rats transplanted with differentiated CM-iPSCs showed a significantly reduced number of apomorphine-induced rotations 12 weeks after engraftment, when compared to the non-transplanted rats ($p \leq 0.05$, $p \leq 0.05$, $p \leq 0.01$, compared to non-transplanted rats at 12, 16 and 24 weeks respectively) (Fig. 6B). Grafts were analyzed histologically 6 months after transplantation. All the transplanted animals had surviving grafts (Fig. 6D–E) with partial reinnervation of the host striatum (Fig. 6F–H) as revealed by immunohistochemistry for TH. Neither tumor formation (Fig. 6C–E) nor inflammatory reactions (Fig. 6G) were detected in transplanted animals up to six months after transplantation.

Discussion

Transplantation of differentiated cells derived from ESCs presents ethical and safety issues. Immune rejection and risk of tumor formation are considered to be great hurdles in the field of cell transplantation. The brain is described as an immune-privileged transplantation site[27]. However, the concept of the central nervous system (CNS) as an "immune-privileged" organ has been widely challenged[28]. Immune responses occur in the brain in neurodegenerative disorders or after neural transplantation and immunosuppressive treatments do not fully prevent graft rejection[29]. Even in the absence of immune rejection, allografted DA neurons can elicit immune responses, which eventually lead to aberrant synaptic function[30]. Several factors can influence the inflammatory responses to neural grafts, including the immunological properties of the transplanted cells, the degree of immunological disparity between donor and recipient, cell preparation and implantation techniques[31].

Data on immunological features of human and murine ESCs and their differentiated derivatives are still limited[32]. Undifferentiated ESCs have been considered as immune privileged since they express low levels of human leukocyte antigen class I, and have no expression of class II[33, 34]. However, ESCs lose such immunoprivilege under inflammatory conditions and during differentiation[33]. The risk of immune rejection and the ethical

concerns of ESC have encouraged the development of strategies for the derivation of patient-specific pluripotent stem cells[35, 36]. In principle, iPSCs would be fully compatible with the donor and would allow safe autologous transplants without the need of intensive immunosuppressive regimen for human cell therapy applications.

For these and other reasons, the immunological properties of iPSC lines need to be investigated prior to clinical use. Theoretically, the expression of exogenous transcription factors that drives cell reprogramming could re-induce the expression of embryonic cryptic antigens. Such non-mutated self-protein antigens, derived from stem cells, in such a scenario could theoretically gain immunogenicity and trigger immune recognition even in autologous settings. In vitro differentiation of pluripotent stem cells may also modify the expression signature of immunological antigens and other molecules that participate in immune responses.

The feasibility of a large-scale production and the clinical use of patient-specific iPSCs has being considered[4]. A databank of histocompatible, fully characterized and clinically approved iPSCs and ESCs, generated under Good Manufacturing Practice, would be of great value in order to evaluate stem cell-based therapies in clinical trials. The first necessary step toward the clinical use of histocompatible iPSCs will be to test their safety (tumorigenicity and immunogenicity), and their functional relevance in NHP models. However, immune responses in NHP have always been difficult to investigate because of the high heterogeneity of macaque MHC genes that determines quantitative and qualitative differences. Mauritian CM are the only NHP with fully characterized MHC class I and II immunogenetics[21]. CM therefore represent a valuable model for cell transplantation research.

In the present work, we accomplished the derivation of several MHC-defined CM-iPSC lines. In order to establish a histocompatible iPSC collection, we genotyped 25 Mauritian CM and one Indonesian CM using microsatellite-based PCR. Using retroviral infection of skin dermal fibroblasts with the 4 factors Oct4, Sox2, Klf4 and c-Myc, we generated several histocompatible iPSCs. These lines formed teratomas upon transplantations under the kidney capsule of NOD-SCID mice.

In order to characterize the immunological properties of CM-iPSCs for in vivo applications, we analyzed the surface expression of immune markers (MHC class I and II, NK receptor CD16) on undifferentiated iPSCs in standard growth conditions or upon treatment with IFN-γ, and at different stages of neuronal differentiation. We show that CM-iPSCs express very low levels of MHC-I at basal conditions. Treatment with IFN-γ and neural/neuronal differentiation induced an increase of MHC-I expression. Interestingly, regardless of their prior in vitro characterization (in vitro pluripotency markers and teratoma formation, expression of viral transgenes or propensity to neuronal differentiation), our analysis revealed consistent differences among different lines. For example, CM-iPSC MF 25-04 presented very low levels of MHC-I even after IFN-γ treatment or neuronal differentiation.

All CM-IPSC lines differentiated into midbrain-like DA neurons after applying a protocol favoring such differentiation[13]. When transplanted into the striatum of naïve or 6-OHDA lesioned rats, CM-iPSCs generated neuronal grafts with no sign of immune rejection. Transplanted rats were immunosuppresed with Cyclosporine A (CsA). CsA is a widely used immunosuppressive drug that suppresses the adaptive immune system by interfering with T cell signaling by blocking IL-2 synthesis through inhibition of the calcineurin pathway[37]. However, in CsA-treated rats immune reactions such as microglia activation and CD4+/CD8+ lymphocyte infiltration, can still compromise the survival of discordant xenografts[38, 39]. Moreover, natural cytotoxic activity is not suppressed by CsA. NK-cell

response could be a risk for transplanted neurons that express low levels of MHC molecules[40]. Therefore, the in vivo bioassay described in the current work provides the opportunity to evaluate the immunogenicity of iPSC-derived neuronal grafts. Despite the increase of the expression of MHC-I molecules after neuronal differentiation and cytokine treatment in vitro, the transplantation of differentiated neurons from CM-iPSCs did not induce the activation of the host innate and adaptive immune system. The presence of surviving grafts in all transplanted animals and the absence of T-cell infiltration and microglia activation suggest the low immunogenicity of CM-iPSC-derived neurons.

Importantly, no evidence of overgrowth or tumor was found up to six months after transplantation. In accordance with these findings, neither Ki-67$^+$ proliferating cells nor residual Oct4$^+$ cells were found within the grafts 16 weeks post-transplantation. Grafted cells displayed a pattern of neuronal outgrowth and targeting of distant areas 4 weeks after transplantation. Such neuronal outgrowth was very similar to the outgrowth of DA neurons derived from human iPSCs derived from idiopathic PD patients[23]. We also demonstrated that differentiated CM-iPSCs transplanted into a model of PD had surviving midbrain-like DA neurons that reinnervated the host striatum and induced partial behavioral recovery.

Previously published clinical and experimental data show that rejection, inflammatory reaction and immunization to allografts may occur in neural transplants[41, 42]. While allogenic neural grafts are expected to induce a chronic inflammatory response and cytokine production, which can interfere with the functional engraftment of transplanted neurons[30, 43, 44], autologous and MHC-matched iPSC-derived neurons would theoretically provide survival in the host without any rejection or inflammation around the cells and synapses.

The results of this study demonstrate that functional DA neurons can be derived from MHC-typed primate iPSCs. Transplanted DA neurons from primate ESCs have been previously shown to improve symptoms in a primate model of PD[45]. Further studies will be needed to address long-term safety and efficacy of iPSC-derived neurons in parkinsonian CM. Our ongoing studies in MPTP-treated CM are evaluating functional engraftment, potential for tumor formation and immunological reactions of autologous, MHC-matched and MHC-mismatched iPSC-derived DA neurons.

Conclusion and Summary

In summary, we generated several histocompatible CM-iPSCs and characterized their immunological features. We show that CM-iPSCs express very low levels of immunomodulatory markers (MHC-I, MHC-II and CD16). Neuronal differentiation and pro-inflammatory conditions induced an increase of immune marker expression. Interestingly, our analysis revealed some differences in the immune properties among different lines. Any functional role of such differences, particularly for in vivo settings, deserves further investigation. We demonstrate that DA neurons from CM-iPSCs engraft in the immunosuppressed host striatum of a rodent model of PD, and generate functional grafts without tumor formation or long-term immune reaction. We believe that these CM-iPSCs provide a valuable resource for future pre-clinical investigations in the field of regenerative medicine.

Supplementary Material

Refer to Web version on PubMed Central for supplementary material.

Acknowledgments

We would like to thank Tana Brown, Andrew Kartunen, Kristen Lee, Elizabeth Marlow and Alyssa Yow for excellent technical help. This study was supported by grants to O.I. from the Udall Parkinson`s Disease Center of Excellence Grant P50 NS39793, Department of Defense (WX81XWH-11-1-0069), Poul Hansen Family, Orchard Foundation, the Consolidated Anti-Aging Foundation and the Harold and Ronna Cooper Family; postdoctoral fellowship HA5589/1-1 from the Deutsche Forschungsgemeinschaft (to G.H.), and Training Award T32AG000222-17 from the National Institute on Aging (to T.O.).

References

1. Takahashi K, Tanabe K, Ohnuki M, et al. Induction of pluripotent stem cells from adult human fibroblasts by defined factors. Cell. 2007; 131:861–872. [PubMed: 18035408]
2. Yu J, Vodyanik MA, Smuga-Otto K, et al. Induced pluripotent stem cell lines derived from human somatic cells. Science (New York, N.Y. 2007; 318:1917–1920.
3. Park IH, Zhao R, West JA, et al. Reprogramming of human somatic cells to pluripotency with defined factors. Nature. 2008; 451:141–146. [PubMed: 18157115]
4. Nakatsuji N, Nakajima F, Tokunaga K. HLA-haplotype banking and iPS cells. Nature biotechnology. 2008; 26:739–740.
5. Bontrop RE. Non-human primates: essential partners in biomedical research. Immunological reviews. 2001; 183:5–9. [PubMed: 11782243]
6. Hantraye P, Brownell AL, Elmaleh D, et al. Dopamine fiber detection by [11C]-CFT and PET in a primate model of parkinsonism. Neuroreport. 1992; 3:265–268. [PubMed: 1515582]
7. Mee ET, Badhan A, Karl JA, et al. MHC haplotype frequencies in a UK breeding colony of Mauritian cynomolgus macaques mirror those found in a distinct population from the same geographic origin. Journal of medical primatology. 2009; 38:1–14. [PubMed: 19018947]
8. Wiseman RW, Wojcechowskyj JA, Greene JM, et al. Simian immunodeficiency virus SIVmac239 infection of major histocompatibility complex-identical cynomolgus macaques from Mauritius. Journal of virology. 2007; 81:349–361. [PubMed: 17035320]
9. Jenkins BG, Sanchez-Pernaute R, Brownell AL, et al. Mapping dopamine function in primates using pharmacologic magnetic resonance imaging. J Neurosci. 2004; 24:9553–9560. [PubMed: 15509742]
10. Astradsson A, Jenkins BG, Choi JK, et al. The blood-brain barrier is intact after levodopa-induced dyskinesias in parkinsonian primates--evidence from in vivo neuroimaging studies. Neurobiology of disease. 2009; 35:348–351. [PubMed: 19501164]
11. Sonntag KC, Pruszak J, Yoshizaki T, et al. Enhanced yield of neuroepithelial precursors and midbrain-like dopaminergic neurons from human embryonic stem cells using the bone morphogenic protein antagonist noggin. Stem cells (Dayton, Ohio). 2007; 25:411–418.
12. Wernig M, Zhao JP, Pruszak J, et al. Neurons derived from reprogrammed fibroblasts functionally integrate into the fetal brain and improve symptoms of rats with Parkinson's disease. Proceedings of the National Academy of Sciences of the United States of America. 2008; 105:5856–5861. [PubMed: 18391196]
13. Sanchez-Pernaute R, Lee H, Patterson M, et al. Parthenogenetic dopamine neurons from primate embryonic stem cells restore function in experimental Parkinson's disease. Brain. 2008; 131:2127–2139. [PubMed: 18669499]
14. Chung CY, Seo H, Sonntag KC, et al. Cell type-specific gene expression of midbrain dopaminergic neurons reveals molecules involved in their vulnerability and protection. Human molecular genetics. 2005; 14:1709–1725. [PubMed: 15888489]
15. Livak KJ, Schmittgen TD. Analysis of relative gene expression data using real-time quantitative PCR and the 2(-Delta Delta C(T)) Method. Methods (San Diego, Calif. 2001; 25:402–408.
16. Pruszak J, Ludwig W, Blak A, et al. CD15, CD24, and CD29 define a surface biomarker code for neural lineage differentiation of stem cells. Stem cells (Dayton, Ohio). 2009; 27:2928–2940.
17. Abercrombie. Estimation of nuclear populations from microtome sections. Anat Rec. 1946; 94:239–247. [PubMed: 21015608]

18. Haque NS, LeBlanc CJ, Isacson O. Differential dissection of the rat E16 ventral mesencephalon and survival and reinnervation of the 6-OHDA-lesioned striatum by a subset of aldehyde dehydrogenase-positive TH neurons. Cell transplantation. 1997; 6:239–248. [PubMed: 9171157]
19. Bjorklund LM, Sanchez-Pernaute R, Chung S, et al. Embryonic stem cells develop into functional dopaminergic neurons after transplantation in a Parkinson rat model. Proceedings of the National Academy of Sciences of the United States of America. 2002; 99:2344–2349. [PubMed: 11782534]
20. O'Connor SL, Blasky AJ, Pendley CJ, et al. Comprehensive characterization of MHC class II haplotypes in Mauritian cynomolgus macaques. Immunogenetics. 2007; 59:449–462. [PubMed: 17384942]
21. Pendley CJ, Becker EA, Karl JA, et al. MHC class I characterization of Indonesian cynomolgus macaques. Immunogenetics. 2008; 60:339–351. [PubMed: 18504574]
22. Perrier AL, Tabar V, Barberi T, et al. Derivation of midbrain dopamine neurons from human embryonic stem cells. Proceedings of the National Academy of Sciences of the United States of America. 2004; 101:12543–12548. [PubMed: 15310843]
23. Hargus G, Cooper O, Deleidi M, et al. Differentiated Parkinson patient-derived induced pluripotent stem cells grow in the adult rodent brain and reduce motor asymmetry in Parkinsonian rats. Proceedings of the National Academy of Sciences of the United States of America. 2010; 107(36): 15921–15926. [PubMed: 20798034]
24. Liu G, Ma H, Jiang L, et al. Allograft inflammatory factor-1 and its immune regulation. Autoimmunity. 2007; 40:95–102. [PubMed: 17453710]
25. Mendez I, Sanchez-Pernaute R, Cooper O, et al. Cell type analysis of functional fetal dopamine cell suspension transplants in the striatum and substantia nigra of patients with Parkinson's disease. Brain. 2005; 128:1498–1510. [PubMed: 15872020]
26. Ferri AL, Lin W, Mavromatakis YE, et al. Foxa1 and Foxa2 regulate multiple phases of midbrain dopaminergic neuron development in a dosage-dependent manner. Development (Cambridge, England). 2007; 134:2761–2769.
27. Barker CF, Billingham RE. Immunologically privileged sites. Advances in immunology. 1977; 25:1–54. [PubMed: 345773]
28. Galea I, Bechmann I, Perry VH. What is immune privilege (not)? Trends in immunology. 2007; 28:12–18. [PubMed: 17129764]
29. Barker RA, Widner H. Immune problems in central nervous system cell therapy. NeuroRx. 2004; 1:472–481. [PubMed: 15717048]
30. Soderstrom KE, Meredith G, Freeman TB, et al. The synaptic impact of the host immune response in a parkinsonian allograft rat model: Influence on graft-derived aberrant behaviors. Neurobiology of disease. 2008; 32:229–242. [PubMed: 18672063]
31. Cooper O, Astradsson A, Hallett P, et al. Lack of functional relevance of isolated cell damage in transplants of Parkinson's disease patients. Journal of neurology. 2009; 256(Suppl 3):310–316. [PubMed: 19711122]
32. Saric T, Frenzel LP, Hescheler J. Immunological barriers to embryonic stem cell-derived therapies. Cells, tissues, organs. 2008; 188:78–90. [PubMed: 18303241]
33. Drukker M, Katz G, Urbach A, et al. Characterization of the expression of MHC proteins in human embryonic stem cells. Proceedings of the National Academy of Sciences of the United States of America. 2002; 99:9864–9869. [PubMed: 12114532]
34. Li L, Baroja ML, Majumdar A, et al. Human embryonic stem cells possess immune-privileged properties. Stem cells (Dayton, Ohio). 2004; 22:448–456.
35. Park IH, Arora N, Huo H, et al. Disease-specific induced pluripotent stem cells. Cell. 2008; 134:877–886. [PubMed: 18691744]
36. Soldner F, Hockemeyer D, Beard C, et al. Parkinson's disease patient-derived induced pluripotent stem cells free of viral reprogramming factors. Cell. 2009; 136:964–977. [PubMed: 19269371]
37. Liu J, Farmer JD Jr, Lane WS, et al. Calcineurin is a common target of cyclophilin-cyclosporin A and FKBP-FK506 complexes. Cell. 1991; 66:807–815. [PubMed: 1715244]
38. Pakzaban P, Deacon TW, Burns LH, et al. A novel mode of immunoprotection of neural xenotransplants: masking of donor major histocompatibility complex class I enhances transplant survival in the central nervous system. Neuroscience. 1995; 65:983–996. [PubMed: 7617173]

39. Galpern WR, Burns LH, Deacon TW, et al. Xenotransplantation of porcine fetal ventral mesencephalon in a rat model of Parkinson's disease: functional recovery and graft morphology. Experimental neurology. 1996; 140:1–13. [PubMed: 8682173]
40. Dressel R, Nolte J, Elsner L, et al. Pluripotent stem cells are highly susceptible targets for syngeneic, allogeneic, and xenogeneic natural killer cells. Faseb J. 2010; 24:2164–2177. [PubMed: 20145206]
41. Widner H, Brundin P, Bjorklund A, et al. Survival and immunogenicity of dissociated allogeneic fetal neural dopamine-rich grafts when implanted into the brains of adult mice. Exp Brain Res. 1989; 76:187–197. [PubMed: 2753100]
42. Widner H, Brundin P. Sequential intracerebral transplantation of allogeneic and syngeneic fetal dopamine-rich neuronal tissue in adult rats: will the first graft be rejected? Cell transplantation. 1993; 2:307–317. [PubMed: 8162272]
43. Freed CR, Greene PE, Breeze RE, et al. Transplantation of embryonic dopamine neurons for severe Parkinson's disease. The New England journal of medicine. 2001; 344:710–719. [PubMed: 11236774]
44. Mirza B, Krook H, Andersson P, et al. Intracerebral cytokine profiles in adult rats grafted with neural tissue of different immunological disparity. Brain Res Bull. 2004; 63:105–118. [PubMed: 15130699]
45. Takagi Y, Takahashi J, Saiki H, et al. Dopaminergic neurons generated from monkey embryonic stem cells function in a Parkinson primate model. J Clin Invest. 2005; 115:102–109. [PubMed: 15630449]

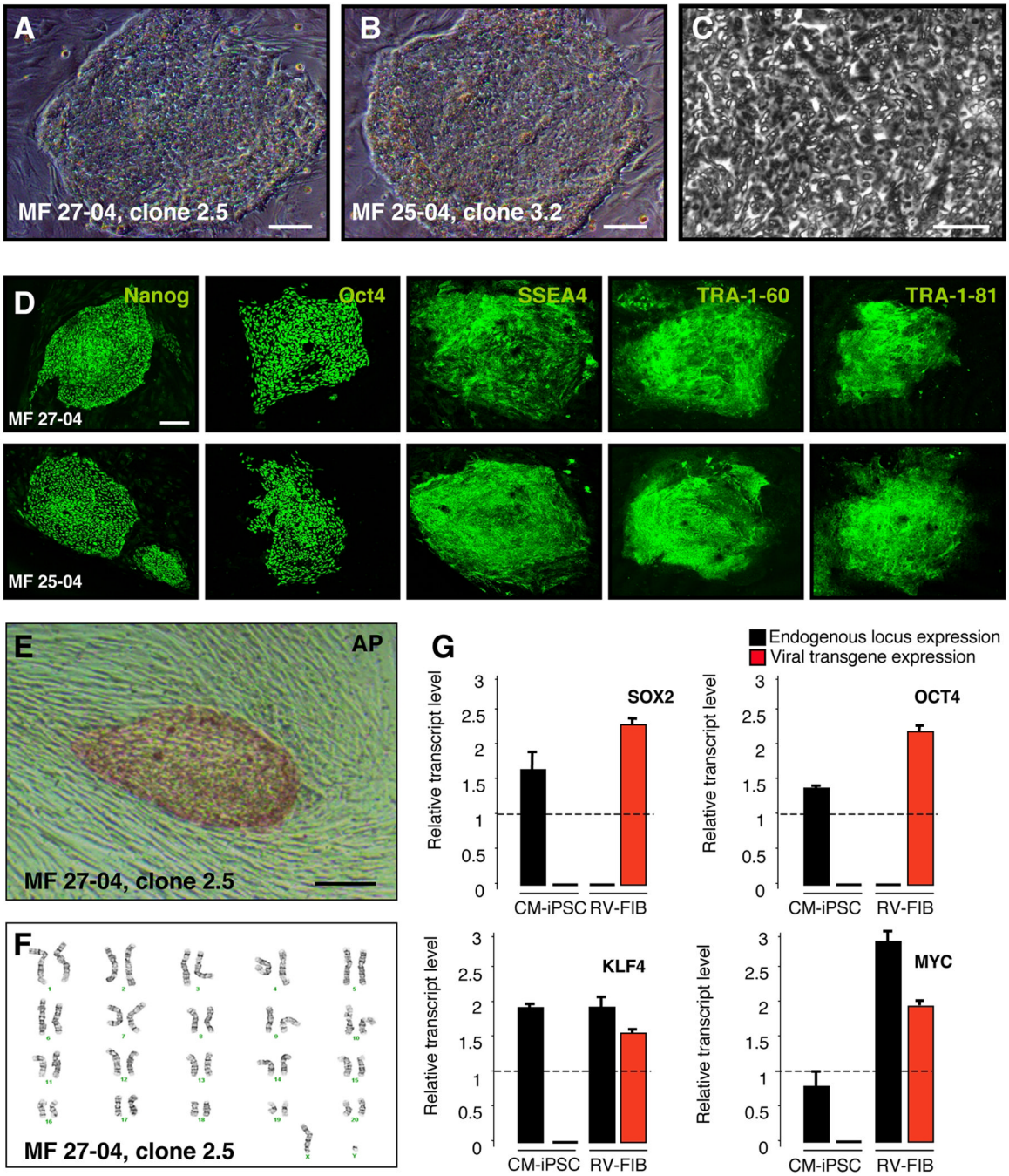

Figure 1. Generation of Cynomolgus Monkey iPSC

(A–B) Phase contrast images showing ESC-like morphology of CM-iPSCs on MEF. **(C)** High-magnification image of CM-iPSCs showing the high nucleus/cytoplasm ratio and prominent nucleoli. **(D)** Immunofluorescence staining for the pluripotency markers Nanog, Oct4, SSEA-4, TRA-1–60, and TRA-1–81. **(E)** CM-iPSC colonies stained positive for alkaline phosphatase (AP). **(F)** Karyotype analysis of CM-iPSCs (line 27-04, passage 10). CM-iPSCs maintained a normal 42, XY karyotype after expansion.**(G)** Quantitative RT-PCR showing induction of endogenous transcripts of Sox2, Oct4, Klf4, and c-Myc. Primers specific for endogenously (black) or viral exogenous (red) encoded transcripts of the four

reprogramming factors. Monkey dermal fibroblasts, four days after transduction with the four retroviruses (RV-FIB), were used as a positive control for expression of the viral transgenes. Values were normalized by the averaged value of β-actin. Values are expressed as averages + SEM of 3 independent experiments. The value of hESCs (H9) was set to 1 in each experiment. Scale bar, 200 μm (A–B, D–E); 20 μm (C).

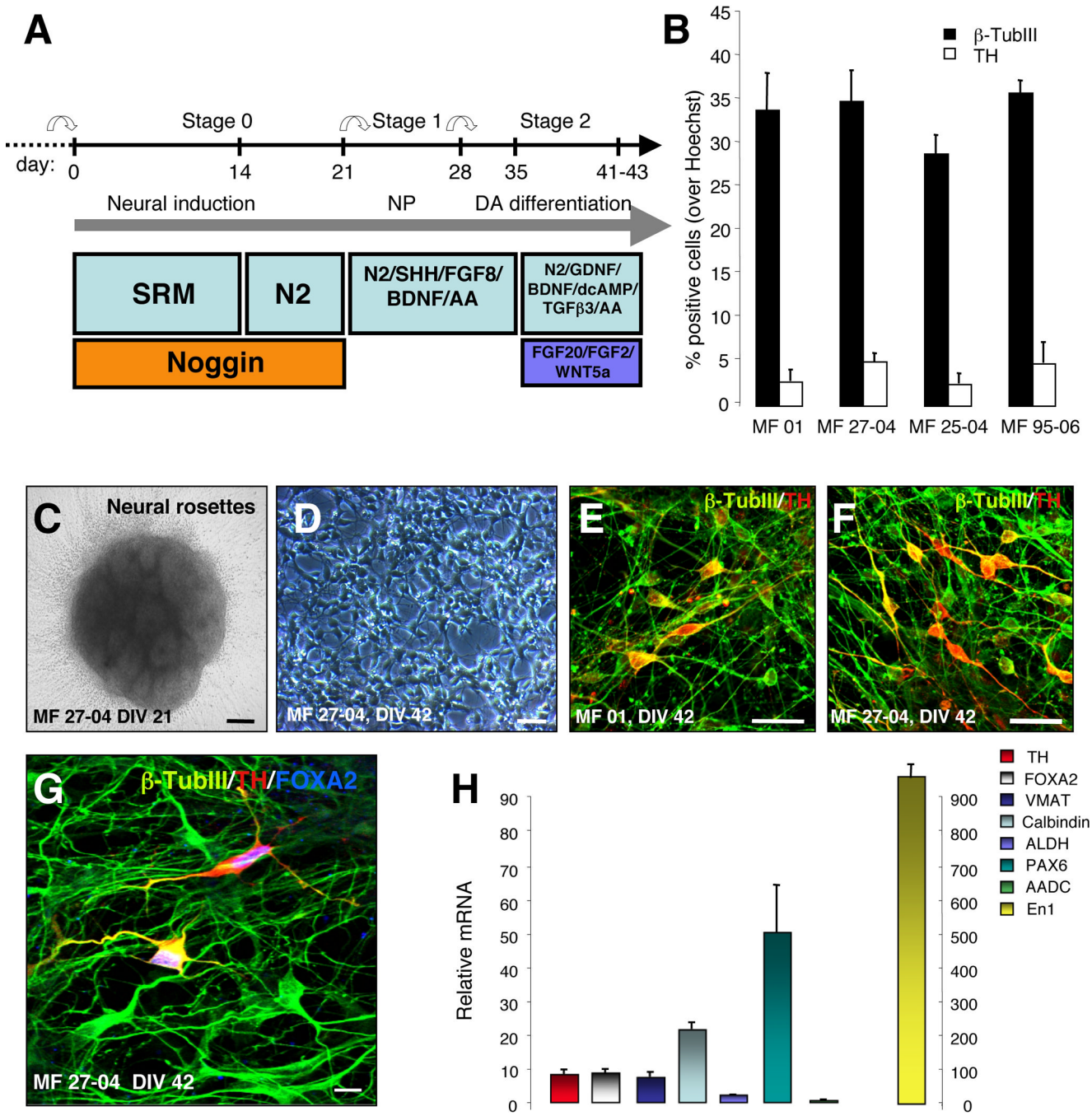

Figure 2. Generation of DA neurons from CM-iPSCs

(A) Schematic representation of the in vitro differentiation protocol. **(B)** Graphs indicate the percentage of cells that stained positive for β-TubIII and TH relative to nuclear Hoechst staining. Values are expressed as averages + SEM of 3 independent experiments. **(C)** Neural rosettes derived from CM-iPSCs (DIV 21). **(D)** Differentiated neurons derived from CM-iPSCs (DIV 42). **(E–F)** Immunofluorescence staining of neuronal cultures derived from CM-iPSCs (lines MF 01, MF 27-04) for β-TubIII (green) and TH (red). **(G)** Confocal images of neuronal cultures stained for β-TubIII (green), TH (red) and Foxa2 (blue). **(H)** Quantitative RT-PCR analysis of midbrain transcription factors, DA neurotransmission

markers (TH, Foxa2, VMAT, ALDH, Nurr1, En1, AADC, Pax6) and Calbindin in differentiated iPSCs. cDNA was isolated from differentiated iPSCs, and values were normalized to the level of β-actin. Values represent mean + SEM. Three independent experiments were performed in triplicate. Scale bar: 50 μm (C–D); 20 μm (E–G).

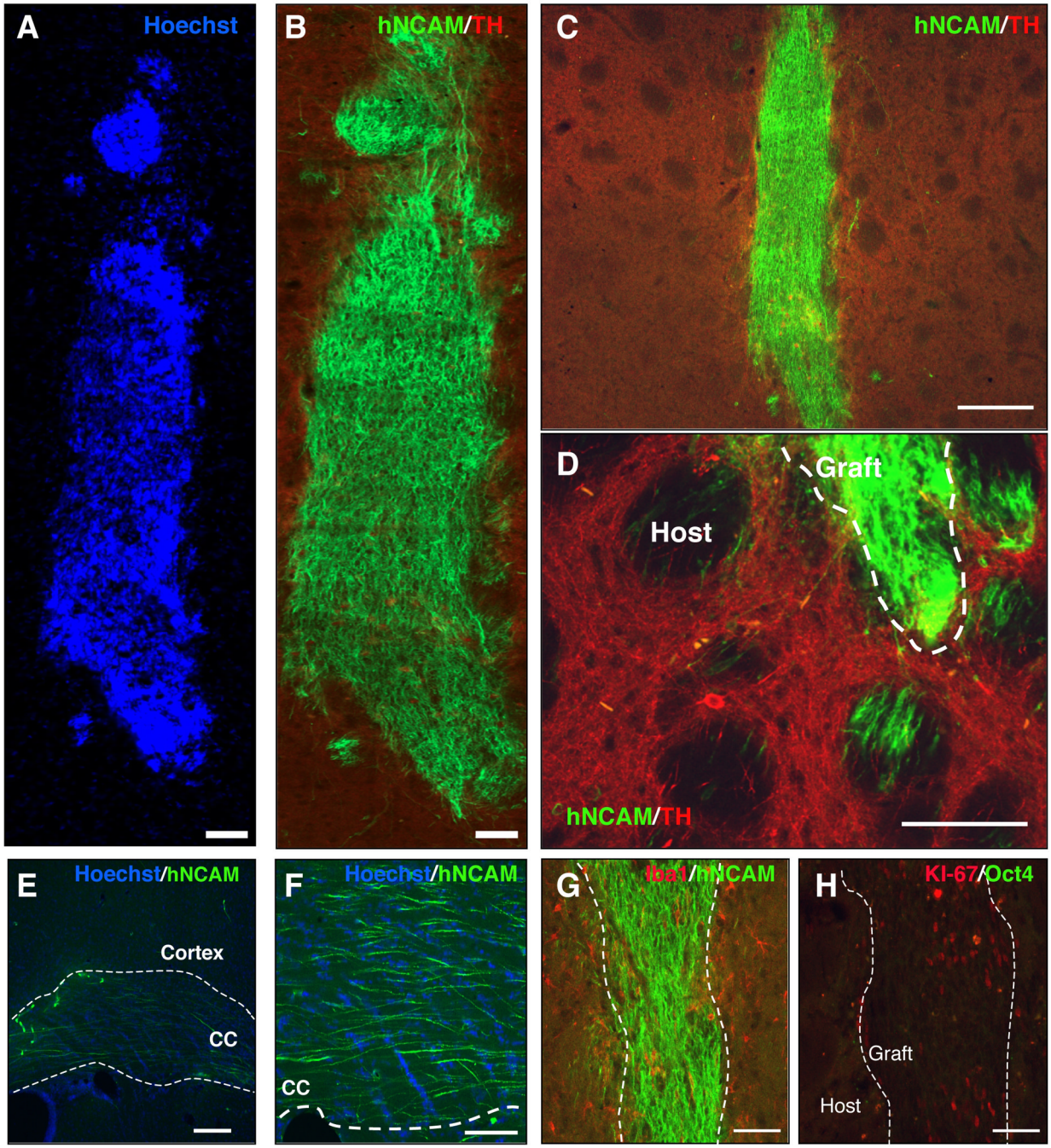

Figure 3. Transplantation of CM-iPSC-derived neurons into the adult striatum of naïve rats

CM-iPSCs (line MF 01) were differentiated into DA neurons and 200,000 cells were transplanted into the right striatum of unlesioned rats under immunosuppression. Grafts were analyzed 4 weeks after the transplantation. **(A–B)** Confocal reconstruction of a representative graft stained for the human/primate-specific neural cell adhesion molecule (NCAM) (green) and TH (red). Nuclei are counterstained with Hoechst. **(C)** Lower magnification of the graft. **(D–F)** Photomicrographs of NCAM-stained brain sections 4 weeks after transplantation showing axonal outgrowth of NCAM+ neurons from the graft into the host striatum, along the white matter tracts (corpus callosum) and cerebral cortex.

(G) Immunostaining for hNCAM (green) and the microglial marker Iba1 (red) revealed the absence of microglial reaction. **(H)** Immunostaining for the proliferative marker Ki-67 (red) and Oct4 (green) showing the presence of a low percentage of Ki-67+/Oct4- cells within the graft. Scale bar: 100 μm (A–B,D and F-H), 200 μm (C,E).

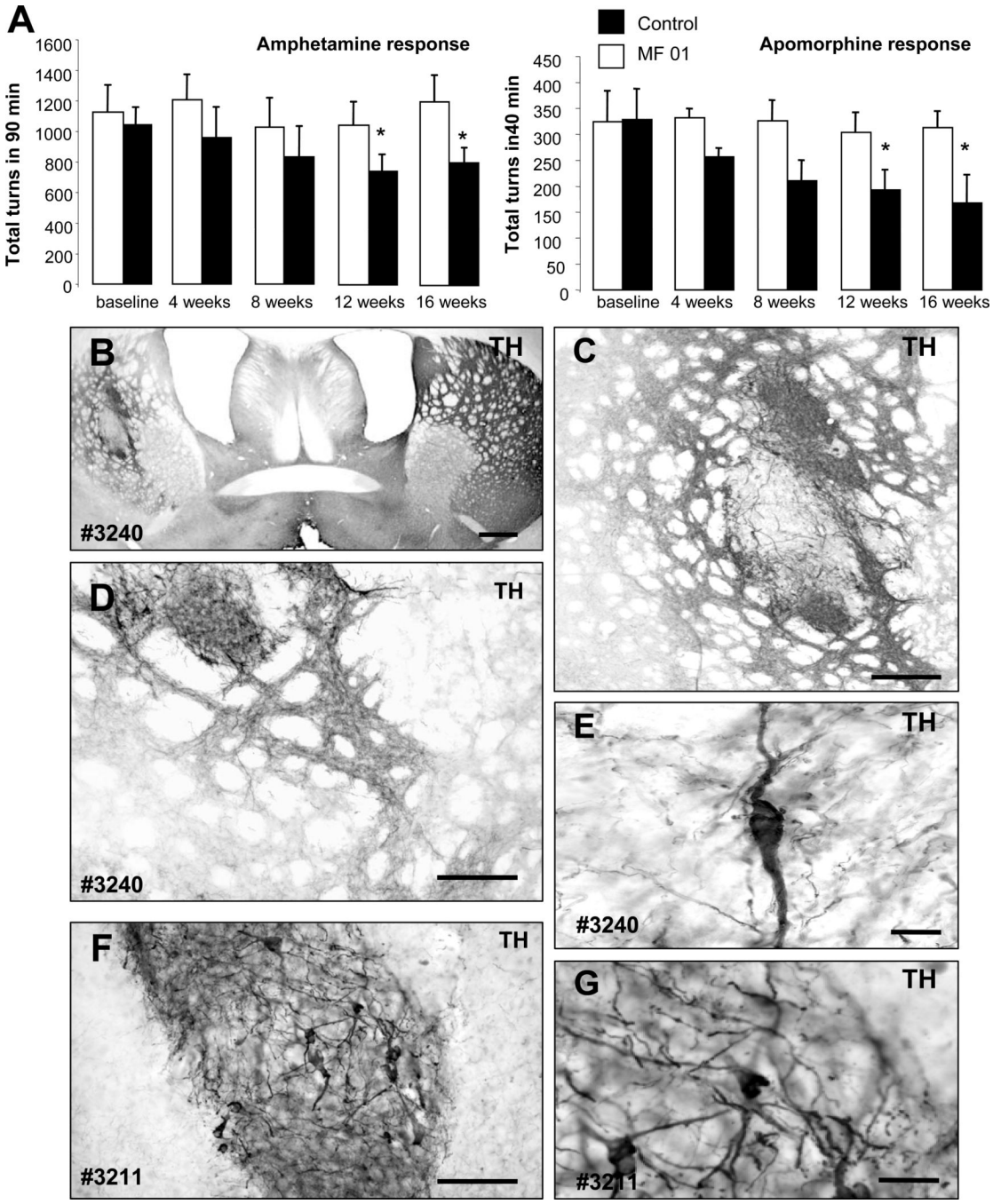

Figure 4. CM-iPSC-derived neurons improve behavioral deficits of parkinsonian rats

(A) CM-iPSCs (line MF-01) were differentiated into DA neurons and 400,000 cells were transplanted into the right striatum of 6OHDA-lesioned rats under immunosuppression. Amphetamine and apomorphine response were examined before and at 4, 8, 12 and 16 weeks post-transplantation. Animals showed a progressive reduction in the response compared to pre-transplantation scores. (Transplanted animals n=9, lesion only animals n=4; *, p <0.05 ANOVA repeated-measures over time). **(B–G)** Tyrosine hydroxylase (TH) immunoreactivity in representative grafts (rat #3211, #3240) derived from differentiated

primate iPSCs showing TH + neurons within the graft and areas of dense TH neuritic arborization. Scale bar: 200 μm (B–D); 50 μm (F), 20 μm (E–G).

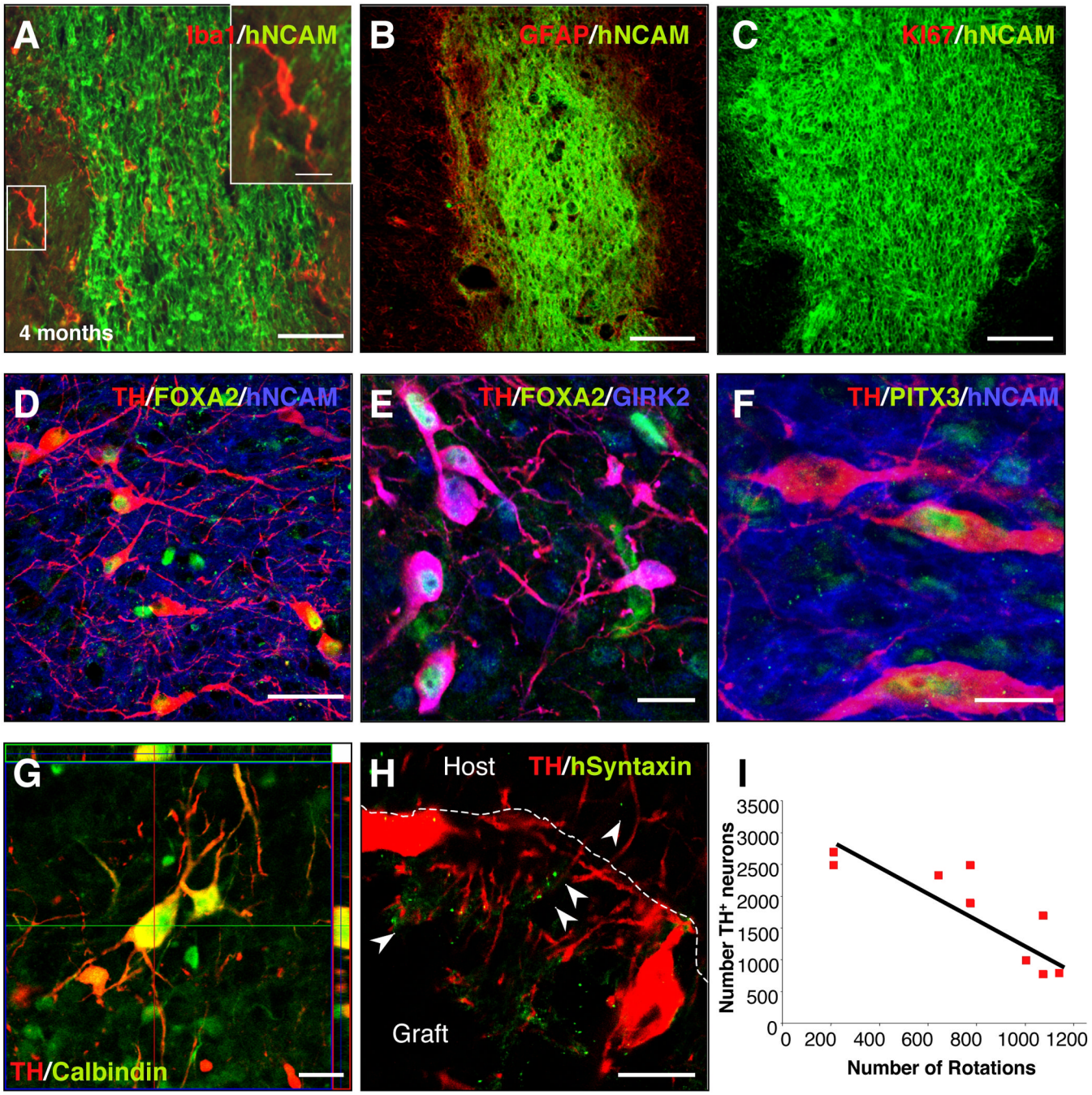

Figure 5. Analysis of neuronal grafts

Confocal analysis of CM-iPSC-derived grafts, 16 weeks post-transplantation. **(A)** Staining for the microglial marker Iba1 showed the absence of activated microglial cells around the grafts. The insert shows high magnification of microglial cells with a resting phenotype. **(B)** Staining for the astrocytic marker GFAP revealed the absence of astrogliosis around the grafts. **(C)** Staining for the proliferation marker Ki-67 showing absence of proliferating cells 16 weeks after transplantation. **(D–F)** Confocal analysis of iPSC grafts showed that most grafts contained midbrain-like DA neurons. The grafted TH+ cells (red) were colabeled with antibodies against human NCAM (blue) (D–F), FOXA2 (green) (D–E), GIRK2 (blue) (E),

Pitx3 (green) (F). **(G)** Confocal images showing TH+ neurons (red) in a representative graft co-expressing the calcium-binding protein calbindin (red). **(H)** Confocal images showing the localization of human syntaxin within the graft and in the host striatum. **(I)** Correlation between number of TH+ neurons and number of rotations (n=9; simple regression, r=0.885, r^2=0.784, P=0.01). Scale bar: 100 μm (A–D), 50 μm (A–E), 20 μm (F–I).

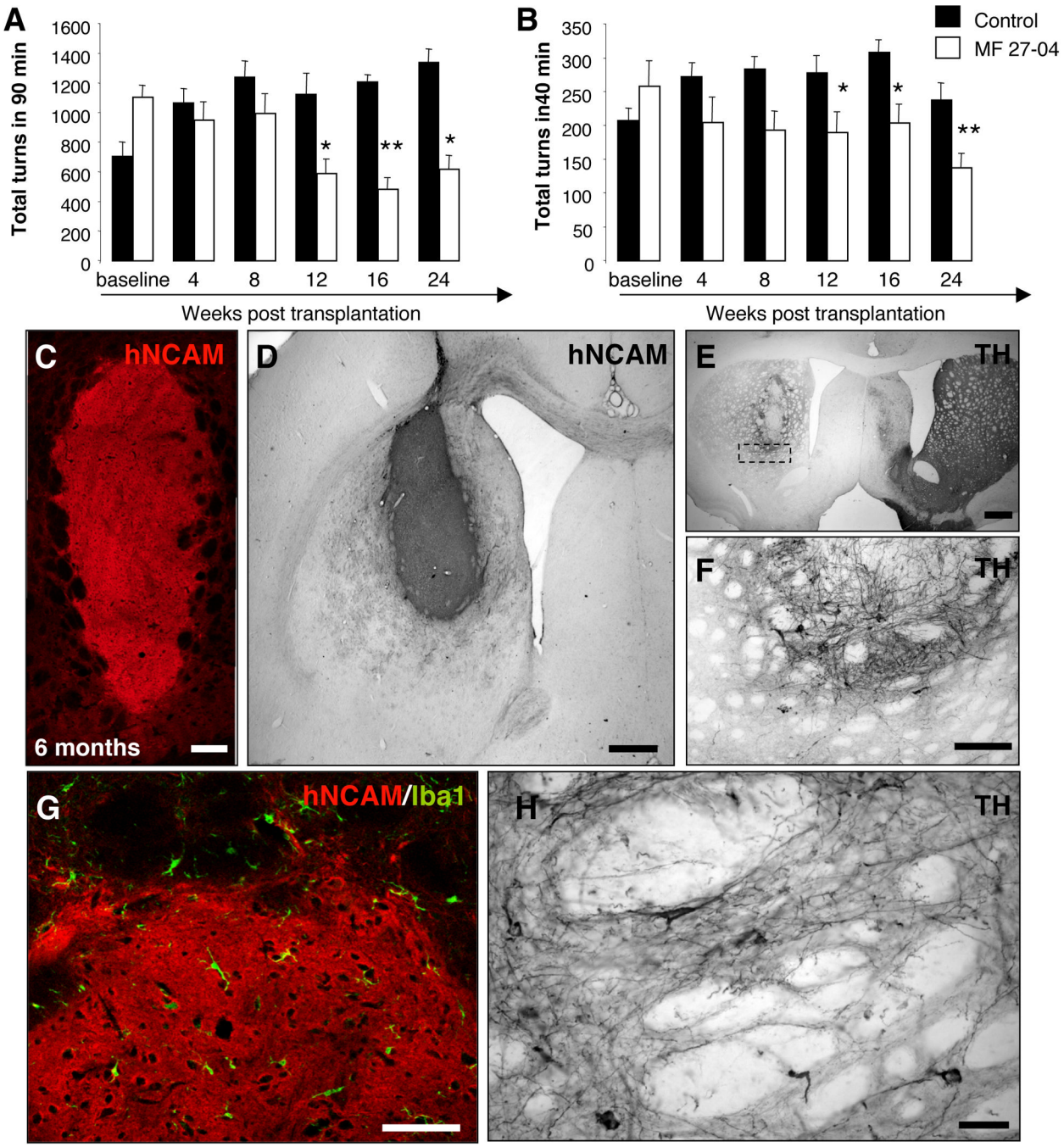

Figure 6. Long-term analysis of neuronal grafts

CM-iPSCs (line MF 27-04) were differentiated into DA neurons and 400,000 cells were transplanted into the right striatum of 6-OHDA-lesioned rats. **(A–B)** Amphetamine and apomorphine response were examined before and at 4, 8, 12, 16, and 24 weeks post-transplantation. Animals showed a progressive reduction in the response compared to pre-transplantation scores. (Transplanted animals n=11, lesion only animals n=6; *, $p < 0.05$; **, $p < 0.01$, ANOVA repeated-measures over time). **(C)** Confocal reconstruction of a representative graft stained for the hNCAM (red). **(D)** NCAM immunoreactivity in a representative graft. **(E–F,H)** TH immunoreactivity in representative grafts showing survival

of TH+ neurons and neuritic arborization. **(G)** Staining for the microglial marker Iba1 showed the absence of activated microglial cells around the grafts. Scale bar: 100 μm (B–C,G), 200 μm (E), 20 μm (F, H).